Ultrasonics Sonochemistry 76 (2021) 105650

Contents lists available at ScienceDirect

Ultrasonics Sonochemistry

journal homepage: www.elsevier.com/locate/ultson

Isothermal and temperature-cycling retrogradation of high-amylose corn starch: Impact of sonication on its structural and retrogradation properties

Kyu Tae Han [a,1], Ha Ram Kim [a,b,1], Tae Wha Moon [a,*], Seung Jun Choi [c,*]

[a] Department of Agricultural Biotechnology, Seoul National University, Seoul 08826, Republic of Korea
[b] Research Group of Food Processing, Research Division of Strategic Food Technology, Korea Food Research Institute, Wanju-gun, Jeollabuk-do 55365, Republic of Korea
[c] Department of Food Science and Technology, Seoul National University of Science and Technology, Seoul 01811, Republic of Korea

ARTICLE INFO

Keywords:
High-amylose corn starch
Sonication
Structural properties
Retrogradation
Avrami kinetics model
Resistant starch

ABSTRACT

In this study, the effects of sonication and temperature-cycled storage on the structural properties and resistant starch content of high-amylose corn starch were investigated. Sonication induced a partial depolymerization of the molecular structures of amylopectin and amylose. Sonication treatment induced the appropriate structural changes for retrogradation. Although the relative crystallinity of sonicated starch was lower than that of non-sonicated starch, sonicated starch after retrogradation showed much higher relative crystallinity than non-sonicated starch. Regardless of sonication treatment, temperature-cycled storage resulted in a higher degree of retrogradation than isothermal storage, but the rate of retrogradation was greater in sonicated starch than in non-sonicated starch, as supported by retrogradation enthalpy, the Avrami constant, and relative crystallinity. The highly developed crystalline structure in sonicated starches due to retrogradation was reflected by the large amount of resistant starch.

1. Introduction

Retrogradation is an unavoidable phenomenon during the cooling and storage of cooked starch or starchy foods. Starch chains in the gelatinized paste reassociate and form a more ordered structure during retrogradation. The degree of retrogradation is influenced by starch concentration and storage conditions (temperature, time, and water content), as well as inherent starch properties (starch crystallinity, ratio of amylose to amylopectin, molecular weight, and botanical origin) [1–4].

Amylose and amylopectin play different roles in retrogradation. Amylose rapidly and irreversibly reassociates to form crystal nuclei in the early stage of retrogradation. Nucleation is known as the rate-determining step of retrogradation [5]. Long-term retrogradation, including propagation and maturation, is observed following nucleation. The crystalline region of amylopectin grows slowly around the amylose crystal nucleus due to the interaction of the outer chains of amylopectin with the amylose nucleus and thus, forms a perfect crystallite. The overall crystallization rate of starch mainly depends on the nucleation and propagation rates [6].

Ordered structures assembled during retrogradation are generally more resistant to enzymatic digestion [7]. The resulting product is resistant starch (RS), which is a portion of starch that cannot be digested by amylases in the small intestine [8]. RS is classified into five sub-categories according to the mechanism of resistance against digestion [9]. RS reaches the colon, where it is fermented to short-chain fatty acids by the microbiota [10] and provides many health benefits to humans, including reducing postprandial blood glucose levels and improving insulin sensitivity [11–13]. RS also helps prevent type 2 diabetes and manage obesity and cardiovascular diseases [14].

Starch characteristics can be altered by physical, chemical, and enzymatic modifications [15,16]. Ultrasound techniques use mechanical waves with frequencies above 16 kHz. Ultrasound techniques have beneficial effects on food processing and preservation, by modifying the composition and structure of products [17]. Physical depolymerization is the main driving force that alters starch structure during sonication. However, unlike other physical modifications, it is accompanied by chemical depolymerization of starch molecules [18]. In particular, radicals (•OH, •O, •HO_2) generated during ultrasonication penetrate the path formed by physical depolymerization and react with covalent bonds in starch molecules. The main result of physical and chemical depolymerization by ultrasonication is the reduction in the starch

* Corresponding authors.
E-mail addresses: twmoon@snu.ac.kr (T.W. Moon), choisj@seoultech.ac.kr (S.J. Choi).
[1] Kyu Tae Han and Ha Ram Kim contributed equally to this work.

https://doi.org/10.1016/j.ultsonch.2021.105650
Received 12 January 2021; Received in revised form 3 June 2021; Accepted 18 June 2021
Available online 21 June 2021

granule size [19] and in the molecular weight of starch molecules [20]. Sonication impacts the water absorption ability and water permeability, resulting in the increase of swelling power and water solubility [21,22], and it allows the alteration of the thermal properties (gelatinization temperature and enthalpy) [21] and pasting profile of starches [22]. Thus, ultrasound treatment can modify the physicochemical and functional characteristics of starches [23]. There are attempts to regulate the digestion properties of starches through ultrasound treatment [24,25]. Due to the ability of ultrasound to modulate the starch structures, there have been attempts to apply ultrasound to the fabrication of starch-based nanoparticles in recent years [26–28].

Meanwhile, a decrease in molecular weight accelerates starch retrogradation [29,30]. Thus, it is hypothesized that the molecular weight reduction due to sonication may increase the degree of retrogradation. However, as Zhu [31] emphasized, the mechanism whereby the molecular changes of starch chains incurred by sonication affect the retrogradation properties of starch has not been comprehensively studied. Therefore, a better understanding of the molecular basis for the effect of sonication on retrogradation is needed.

The objectives of the current study were to investigate the effect of sonication treatment on the structural properties of high-amylose corn starch and to assess its influence on the retrogradation behaviors and resistant starch content of high-amylose corn starch. The present study focused on RS3, which is the enzyme-resistant starch fraction formed by the retrogradation of native and sonicated starches, through isothermal storage and temperature-cycling conditions. This study contributes to our understanding of the structural alterations of starch induced by sonication. In addition, this study will help evaluate the potential for sonicated starches to be used as a novel source of RS.

2. Materials and methods

2.1. Materials

High-amylose corn starch (HYLON V) was obtained from Ingredion (Westchester, IL, USA). According to the manufacturer of HYLON V, it contains approximately 55% amylose. A resistant starch assay kit was purchased from Megazyme (Wicklow, Ireland). All other chemicals were of reagent grade.

2.2. Preparation of sonicated starch

For sonication, high amylose corn starch was suspended into distilled water to 10% (w/w). The sonication was performed using VCX-400 sonicator (Sonics & Materials, Newtown, CT, USA) with a titanium alloy probe (13 mm) with intensity set at 70% (360 W) at intervals of 10 min. The probe was placed in the middle of the starch suspension. Ambient temperature was maintained by immersion in an iced-water bath during sonication. Sonication treatment was performed for 10–60 min as a preliminary test, and starch samples sonicated for 60 min were used for further analysis. Sonicated starch was washed three times with distilled water, which was recovered as precipitant via centrifugation (10,000 × g, 10 min). Lyophilization was employed to remove the water from sonicated starch, and the lyophilized sample was ground into powder using mortar and pestle. The ground powder was passed through a 100-mesh sieve.

2.3. Preparation of starch samples by isothermal and temperature-cycled retrogradation

Sonicated and non-sonicated starch suspensions (20%, w/w) were gelatinized by boiling for 30 min. The gelatinized starch was cooled to room temperature, hermetically sealed, and stored under different temperature conditions: a constant temperature of 4 °C or cycles of 4 °C for 2 days and subsequently, 70 °C for 2 days. After the retrogradation process, each sample was lyophilized, ground, and passed through a 100-mesh sieve.

2.4. Evaluation of thermal transition properties

Thermal transition properties were examined using a differential scanning calorimeter (Diamond DSC; Perkin-Elmer, Waltham, MA, USA). Each sample (10 mg) was weighed in a stainless steel pan, and 30 μL of distilled water was added (starch:water = 1:3 ratio). The sample pan was sealed and kept at room temperature overnight to achieve the even moisture distribution. Sample pans were firstly heated from 20 to 180 °C at a rate of 10 °C/min, and then cooled to −30 °C at a rate of 20 °C/min. After cooling, the second scans were performed from −30 to 40 °C at a rate of 10 °C/min. An empty pan was used as the reference. Peak temperature (T_p) and melting enthalpy (ΔH) were recorded from the first scan. The glass transition temperature (T_g) was obtained from the second scan. The enthalpy of the retrograded samples was plotted following the Avrami kinetics model.

The Avrami equation can be written as follows [32]:

$$\frac{\Delta H_{inf} - \Delta H_t}{\Delta H_{inf} - \Delta H_0} = e^{-k \cdot t^n},$$

where t is the time (days), k is the rate constant (day^{-1}), and n is the Avrami exponent. ΔH_t, ΔH_0, and ΔH_{inf} are endothermic enthalpies (J/g) at times t, 0, and infinity. ΔH_{inf} was obtained after 60 days of retrogradation. The following logarithmic form of this equation was used to analyze the data:

$$\ln\left(\frac{\Delta H_{inf} - \Delta H_t}{\Delta H_{inf} - \Delta H_0}\right) = -k \cdot t^n.$$

2.5. X-ray diffraction patterns and relative crystallinity

X-ray diffraction analysis was performed using a powder X-ray diffractometer (New D8 Advance; Bruker, Karlsruhe, Germany) at 40 kV and 40 mA. Samples were scanned in the diffraction angle (2θ) from 3 to 33°, with a 0.02° step size and a count time of 2 s. Relative crystallinity was calculated according to the following equation:

$$\text{relative crystallinity } (\%) = \frac{A_c}{A_a + A_c} \times 100,$$

where A_a is the area of the amorphous region and A_c is the area of the crystalline region.

2.6. Assay of RS content

An RS assay kit (K-RSTAR; Megazyme) was used to measure RS content. Starch samples (100 mg) were incubated with 4 mL of pancreatic α-amylase (10 mg/mL) containing amyloglucosidase (3 U/mL) as the supplier provided, at 37 °C for 16 h with constant shaking (100 rpm). The reaction was stopped with 4.0 mL of ethanol (99%, v/v) and centrifuged 1500×g for 10 min to recover RS as pellets. Samples were then washed twice with ethanol (50%, v/v) and centrifuged at 1500×g for 10 min. The resulting pellet was then dissolved in 2 M KOH (2 mL) for 20 min. The dissolved pellet was mixed with 1.2 M sodium acetate and hydrolyzed to glucose using 0.1 mL of amyloglucosidase (3,300 U/mL) at 50 °C for 30 min. The hydrolysate was diluted to 100 mL and centrifuged at 1500×g for 10 min. The released glucose was analyzed using a glucose oxidase–peroxidase reagent provided in the assay kit.

3. Results and discussion

3.1. Structural changes in high-amylose corn starch by sonication

Based on the shift in retention times of the amylopectin and amylose

peaks in gel permeation chromatography observed in our preliminary study (Supplementary Fig. 1), physical (or mechanical) and chemical depolymerization during ultrasonication induced a reduction in the molecular weight of high-amylose corn starch as described above [33,34]. Proton nuclear magnetic resonance spectroscopy showed that the proportion of α-1,6 linkages in the total glycosidic linkages gradually increased with sonication time from 0.8 to 1.8 (native to 60 min, Supplementary Table 1). Because the generation of a new α-1,6 linkage was impractical, this result would be entirely due to a reduction in α-1,4 linkages. α-1,4 Linkage may be more vulnerable to the breakdown than α-1,6 linkage when comparing the Gibbs free energy of the α-1,4 linkage (Δ G = −15.5 kJ/mol) and the α-1,6 linkage (Δ G = −7.1 kJ/mol) [35]. This change resulted in a decrease in the average branch chain length of amylopectin from 22.2 to 21.5 for 0–60 min of sonication treatment. The amorphous region is more susceptible than the crystalline region to physical, chemical, and enzymatic degradation [36], and also to ultrasonic-assisted degradation [33]. Therefore, α-1,4 linkages in amylose, which are located along the amorphous region in the form of single helices or random coils, could also be easily degraded. In addition, the breakdown of α-1,4 linkages in amylopectin mainly occurred in the amorphous regions of the amylopectin cluster. A significant decrease in relative crystallinity with increasing sonication time was also clearly observed, as previously reported [22,25].

Of the starch samples sonicated for 10–60 min and stored under the retrogradation conditions applied in this study, those sonicated for 60 min showed the most significant difference in structural properties and RS content compared with retrograded native starch. Therefore, high-amylose corn starch sonicated for 60 min was used in this study.

3.2. Effects of sonication and retrogradation conditions on the thermal transition properties of high-amylose corn starch

Native starch showed three different types of endothermic peaks: a peak due to the melting of amylopectin crystallites (P_{AP}: 77.96 °C and 7.64 J/g for T_p and ΔH, respectively), a peak due to the melting of amylose–lipid complexes (P_{AL}: 97.01 °C and 0.50 J/g for T_p and ΔH, respectively), and a peak due to the melting of amylose crystallites (P_{AM}; 150.26 °C and 1.12 J/g for T_p and ΔH, respectively). In other hand, significantly altered thermal transition properties were observed in sonicated starch. P_{AM} was disappeared, and P_{AP} was shifted to lower temperature (75.62 °C) with decreased meting enthalpy (2.56 J/g). This phenomenon seemed related with the aforementioned structural changes accompanied by the decomposition of α-1,4 linkage in amylose molecules and amylopectin cluster.

Peak I (P_{AP}) was not detected in non-sonicated (NC) and sonicated (SC) starch samples due to the perfect melting of amylopectin crystallites during gelatinization (Table 1). Since amylose crystallites in native starch had T_p values around 150 °C, amylose crystallites would not be melted fully during gelatinization, which would result in an endothermic peak. The amylose crystallites not melted during gelatinization may behave as nuclei during retrogradation. Changes in ΔH according to storage duration reflect the retrogradation phenomenon.

In the case of untreated starch, the T_p values of P_{AP} and P_{AM} rarely changed with retrogradation time (Table 1), but ΔH values gradually increased as a function of retrogradation time (Fig. 1). T_p represents the structural stability of crystallites or the degree of the order of double helices in crystallites [37], and ΔH is mainly attributed to the melting of the double helix and crystal packing [38]. This indicates that the number of double helices in amylose and amylopectin crystallites gradually increased with retrogradation time, and that the number of double

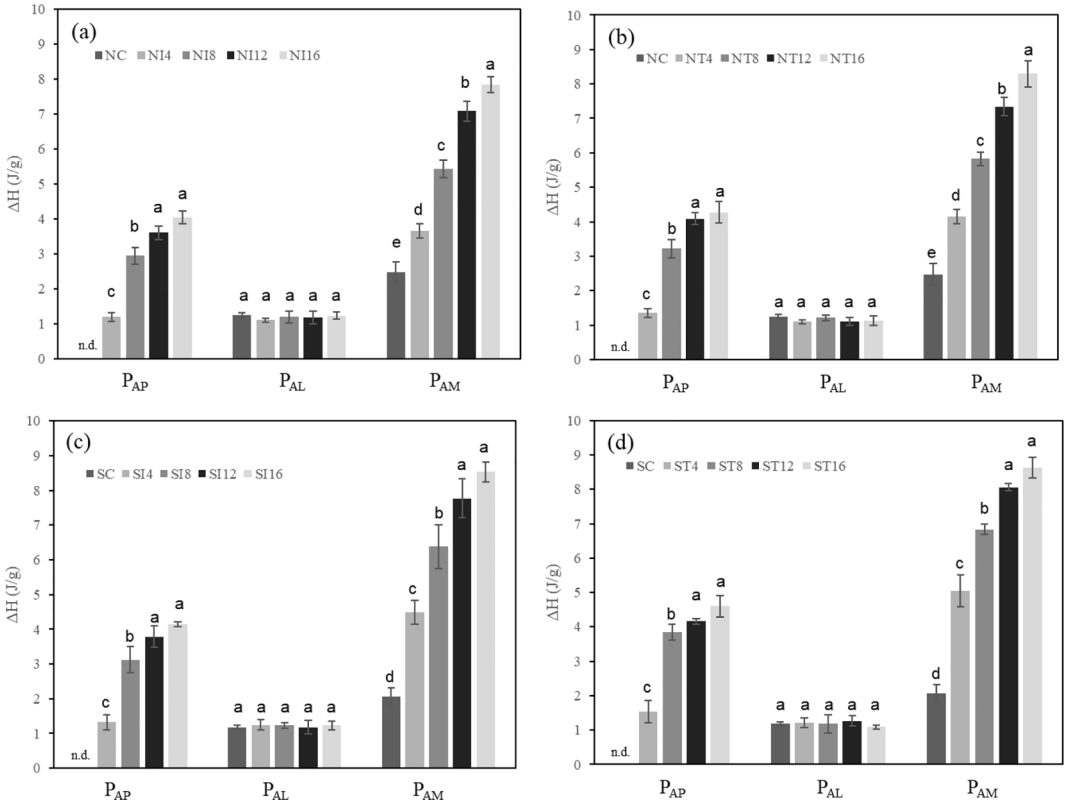

Fig. 1. Changes in melting enthalpies (ΔH) of non-sonicated and sonicated high-amylose corn starches during retrogradation. N, non-sonicated high-amylose corn starch; S, sonicated high-amylose corn starch; C, control (freshly gelatinized); Ix, stored under isothermal conditions for x days; Tx, stored under temperature-cycling conditions for x days. P_{AP}, P_{AL}, and P_{AM} indicate the amylose crystallites, amylose–lipid complexes, and amylose crystallites, respectively. Values with different superscripts in P_{AP}, P_{AL}, or P_{AM} are significantly different ($p \leq 0.05$, Tukey's HSD test).

Table 1
Changes in thermal transition peak temperatures (T_p, °C) of high-amylose corn starch during retrogradation.

Sample	P_{AP} (°C)	P_{AL} (°C)	P_{AM} (°C)	Sample	P_{AP} (°C)	P_{AL} (°C)	P_{AM} (°C)
NC	N.D.	97.17 ± 0.39^{a}	152.81 ± 0.34^{a}	SC	N.D.	97.04 ± 0.30^{ab}	152.67 ± 0.46^{abc}
NI4	59.74 ± 0.69^{a}	96.82 ± 0.35^{a}	$*152.54 \pm 0.42^{a}$	SI4	59.80 ± 0.55^{abc}	96.36 ± 0.51^{b}	$*153.75 \pm 0.47^{a}$
NI8	59.97 ± 0.48^{a}	97.20 ± 0.63^{a}	151.96 ± 0.53^{a}	SI8	60.41 ± 0.72^{a}	96.80 ± 0.58^{b}	152.12 ± 0.17^{bc}
NI12	59.84 ± 0.55^{a}	96.37 ± 0.51^{a}	152.16 ± 0.22^{a}	SI12	59.15 ± 0.29^{bc}	96.42 ± 0.06^{b}	152.36 ± 0.68^{bc}
NI16	59.93 ± 0.52^{a}	96.91 ± 0.56^{a}	152.24 ± 0.50^{a}	SI16	60.12 ± 0.40^{abc}	97.11 ± 0.23^{ab}	151.94 ± 0.13^{c}
NT4	59.98 ± 0.52^{a}	97.09 ± 0.28^{a}	152.61 ± 0.45^{a}	ST4	60.28 ± 0.15^{ab}	96.76 ± 0.36^{b}	153.18 ± 0.22^{ab}
NT8	60.81 ± 0.49^{a}	96.50 ± 0.65^{a}	$*152.19 \pm 0.12^{a}$	ST8	60.21 ± 0.10^{abc}	96.87 ± 0.41^{b}	$*152.92 \pm 0.30^{abc}$
NT12	$*60.38 \pm 0.05^{a}$	97.12 ± 0.60^{a}	152.52 ± 0.15^{a}	ST12	$*59.01 \pm 0.34^{c}$	98.03 ± 0.24^{a}	153.19 ± 0.50^{ab}
NT16	60.28 ± 0.10^{a}	96.71 ± 0.50^{a}	152.30 ± 0.43^{a}	ST16	59.84 ± 0.61^{abc}	97.05 ± 0.40^{ab}	151.80 ± 0.60^{c}

N, non-sonicated high-amylose corn starch; S, sonicated high-amylose corn starch; C, control (freshly gelatinized); Ix, stored under isothermal conditions for x days; Tx, stored under temperature-cycling conditions for x days.
P_{AP}, P_{AL}, and P_{AM} are amylose crystallites, amylose–lipid complexes, and amylose crystallites, respectively.
Values with different superscripts in the same column are significantly different ($p \leq 0.05$, Tukey's HSD test).
An asterisk (*) indicates a significant difference in the peak temperatures for P_{AP}, P_{AL}, and P_{AM} between starches retrograded isothermally and with temperature cycling under the same condition ($p \leq 0.05$, *t*-test).

helices in crystallites increased, without a significant change in their structural stability (the degree of double helix order in crystallites) during retrogradation.

No significant difference was observed in ΔH values between isothermally and temperature-cycled stored starches during the same period (Fig. 2), indicating that the retrogradation temperature had little influence on the increase in the number of double helices in amylose and amylopectin crystallites in untreated starch. Sonicated starch showed a similar pattern in T_p values of P_{AM} and P_{AP}, with negligible difference based on retrogradation temperature. However, their ΔH values increased with storage time, regardless of temperature.

Since starch molecules with low molecular weight easily form crystal nuclei and rapidly develop crystalline structures from these nuclei [39], it was expected that the ΔH values of P_{AM} and P_{AP} for sonicated starch would be greater than those for non-sonicated starch with the same retrogradation time. As shown in Fig. 2, ΔH values of P_{AP} did not show significant differences, while ΔH values of P_{AM} were generally higher in sonicated starches than in non-sonicated starches, when compared with the same period of retrogradation.

Amylose in sonicated starch can be easily reassociated during retrogradation and form double helices, because the mobility of amylose shortened by sonication may be greater than that of amylose in non-sonicated starch. In addition, amylose in sonicated starch was able to form double helices and crystallites, with less structural hindrance, than amylose in non-sonicated starch. Nucleation, the formation of amylose double helices, is the rate-limiting step of starch retrogradation [40,41]

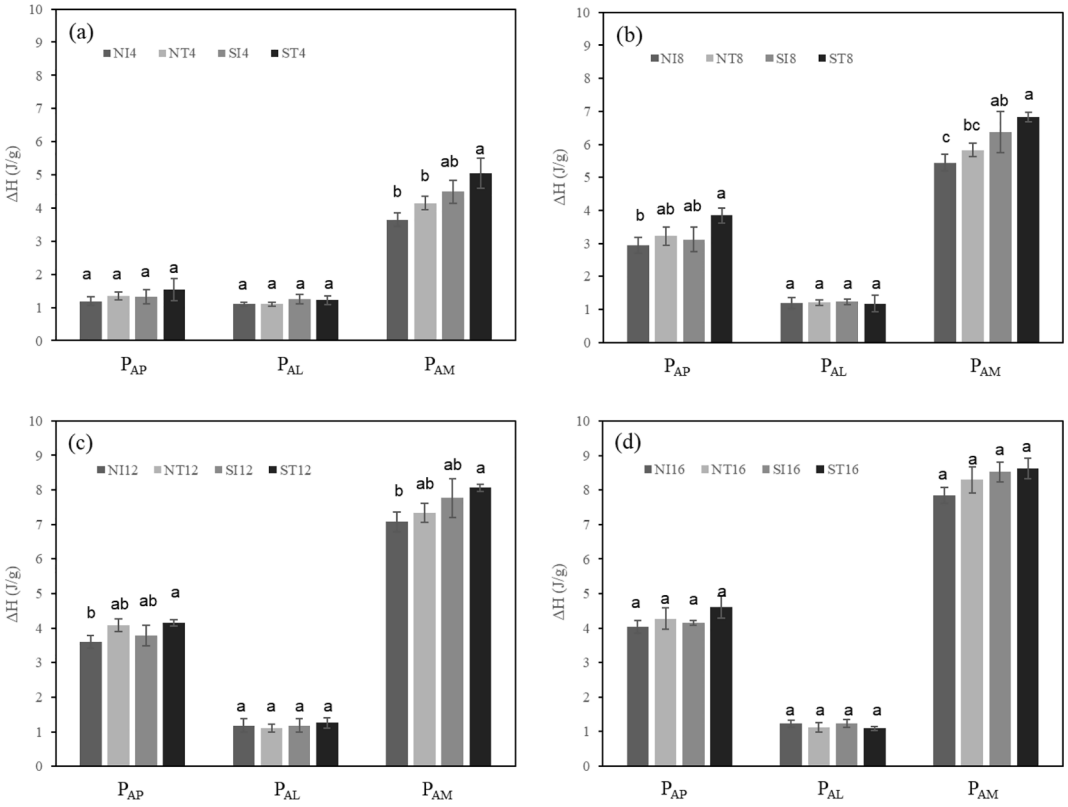

Fig. 2. Comparison of melting enthalpies (ΔH) of non-sonicated and sonicated high-amylose corn starches at the same storage period. N, non-sonicated high-amylose corn starch; S, sonicated high-amylose corn starch; Ix, stored under isothermal conditions for x days; Tx, stored under temperature-cycling conditions for x days. P_{AP}, P_{AL}, and P_{AM} indicate the amylose crystallites, amylose–lipid complexes, and amylose crystallites, respectively. Values with different superscripts in P_{AP}, P_{AL}, or P_{AM} are significantly different ($p \leq 0.05$, Tukey's HSD test).

and thus, the acceleration of nucleation would increase the overall rate of retrogradation, resulting in higher retrogradation enthalpy.

3.3. Impacts of sonication and retrogradation conditions on retrogradation rate of high-amylose corn starch

The kinetics of starch retrogradation (the rate of overall retrogradation) were analyzed using the Avrami kinetics model. The calculated kinetic parameters of retrograded high-amylose corn starch are shown in Table 3. The Avrami kinetics model is based on the premise that crystals nucleate and grow until crystallinity levels off to a constant value. First, the rate constant (k) indicates the overall crystallization rate, because both crystal nucleation and growth rates affect the rate constant. Second, the Avrami exponent (n) depends on two factors: the type of crystal nucleation (instantaneous or sporadic) and the dimensions in which crystal growth takes place (one dimension: rod-like crystals; two dimensions: disc-like crystals; three dimensions: spherulitic crystals) [42]. Starch retrogradation generally results in rod-like crystal growth ($n = 1$) from instantaneous nuclei [29].

The retrogradation of starch occurs through a consecutive three-step process of nucleation, propagation, and maturation, and each step has its own optimum temperature [4]. Temperature cycling storage accelerates the retrogradation of starch by cycling between the optimum temperatures for nucleation and propagation for set periods of time. In general, nucleation is favored near the glass transition temperature of starch molecules, while propagation (crystal growth) and maturation (crystal perfection) are promoted around temperatures that can melt the crystallites [6]. The retrogradation temperatures applied in this study, 4 °C and 70 °C, were the optimal temperatures for the nucleation and propagation of gelatinized starches, respectively.

As shown in Table 2, regardless of temperature, the rate constant (k) of the temperature-cycling stored samples was higher than that of isothermally stored samples. When comparing the effect of sonication, the rate constants (k) of non-sonicated starch (NI and NT) were lower than those of sonicated starch (SI and ST). A significant fissure was found on the surface of amylomaize starch, induced by sonication treatment [33]. This phenomenon promotes molecular leaching from starch granules during gelatinization [43,44]. Therefore, the alignment of starch molecules would be easier compared with untreated starch molecules, resulting in the rapid induction of initial retrogradation. Amylose molecules of sonicated starch were shortened, more readily leached out, and aligned into nuclei formations, resulting in the acceleration of the initial stage of retrogradation. As an indication of the acceleration of initial retrogradation, the gel formed by sonicated starch after gelatinization followed by storage at 4 °C had a higher hardness value than the control sample [45]. The higher ΔH values for P_{AM} of S starches than N starches at the initial retrogradation time (4 days, Fig. 2a) seemed related to this molecular transformation. The results showed that the degree of overall retrogradation also increased in sonicated starches, as supported by the higher k values in SI and ST samples compared with NI and NT samples. This can explain a previous finding that ultrasound treatment increased the setback of starches [22] because setback value is related to short-term retrogradation. The value of the Avrami exponent (n) of all samples was close to 1, which indicated rod-like crystal growth from instantaneous nuclei [29]. Lower n values in sonicated starch indicated more instantaneous retrogradation, supporting the rapid initiation of retrogradation.

Table 2
Parameters of the Avrami kinetics model for retrogradation of starch samples.

Sample group	Avrami kinetics model		
	k (day^{-1})	n	r^2
NI	0.0448^{b}	1.3272^{a}	0.9965
NT	0.0513^{b}	1.3475^{a}	0.9991
SI	0.0712^{a}	1.2728^{a}	0.9998
ST	0.0876^{a}	1.2828^{a}	0.9985

NI, high-amylose corn starch gelatinized and stored under isothermal conditions; NT, high-amylose corn starch gelatinized and stored under temperature-cycling conditions; SI, high-amylose corn starch sonicated, gelatinized, and stored under isothermal conditions; ST, high-amylose corn starch sonicated, gelatinized, and stored under temperature-cycling conditions.
Values with different superscripts for the same starches, retrograded under the same conditions, in the same column are significantly different ($p \leq 0.05$, Tukey's HSD test).

Table 3
Changes in relative crystallinity of non-sonicated and sonicated high-amylose corn starches during retrogradation.

Sample	Relative crystallinity (%)	Sample	Relative crystallinity (%)	t-test
NC	13.17 ± 0.15^{g}	SC	11.43 ± 0.40^{f}	*
NI4	15.60 ± 0.26^{f}	SI4	18.20 ± 0.10^{e}	*
NI8	17.00 ± 0.10^{e}	SI8	19.93 ± 0.15^{d}	*
NI12	18.87 ± 0.15^{c}	SI12	21.40 ± 0.20^{c}	*
NI16	20.47 ± 0.11^{b}	SI16	22.87 ± 0.25^{b}	*
NT4	16.57 ± 0.25^{e}	ST4	19.53 ± 0.15^{d}	*
NT8	18.13 ± 0.25^{d}	ST8	21.77 ± 0.25^{c}	*
NT12	20.23 ± 0.15^{b}	ST12	22.87 ± 0.06^{b}	*
NT16	21.10 ± 0.10^{a}	ST16	24.27 ± 0.21^{a}	*

N, non-sonicated high-amylose corn starch; S, sonicated high-amylose corn starch; C, control (freshly gelatinized); Ix, stored under isothermal conditions for x days; Tx, stored under temperature-cycling conditions for x days.
Values with different superscripts in the same column are significantly different ($p \leq 0.05$, Tukey's HSD test).
An asterisk (*) indicates a significant difference between starches retrograded isothermally and with temperature cycling under the same conditions ($p \leq 0.05$, t-test).

3.4. Influences of sonication and retrogradation conditions on relative crystallinities of high-amylose corn starch

Native starch showed typical B-type crystallites, with a relative crystallinity of approximately 25.97%. Sonication converted the B-type diffraction pattern of native starch to a C-type diffraction pattern, which consisted of a mixture of A- and B-type crystallites, resulting in a significant ($p < 0.05$) decrease in the relative crystallinity of sonicated starch in both the raw and gelatinized states. The significant decrease in crystalline peaks corresponded with previous studies [22,46]. After lyophilization following gelatinization, both non-sonicated and sonicated starches showed similar X-ray patterns of typical amorphous curves from gelatinized starch, with blunt peaks at 17.2°, 20°, and 23° (Fig. 3).

Retrogradation of NC and SC starches resulted in the regeneration of the crystalline structure, which was reflected by the increase in the size of amylose crystal-related major crystalline peaks at 17.2° and 20° with increasing storage duration, leading to an overall increase in relative crystallinity (Table 3). The peak at 5.6° was regenerated only in sonicated starch retrograded for more than 12 days, regardless of storage temperature, whereas it was not observed in non-sonicated starch (Fig. 3). The development of the peak at 5.6° is known to be responsible for amylose crystallites, and it occurred only in sonicated starch during retrogradation, because the decrease in the molecular weight of amylose by sonication caused the formation of amylose crystallites with greater crystallinity, as observed in the DSC analysis. Because of the depolymerization of the α-1,4 linkages, the interaction between amylose and amylopectin or between amylose molecules themselves would be affected [47], which would lead to differences in the mode of packing during retrogradation, i.e., the amylose double helices could be packed into more ordered and perfect crystalline arrangements in sonicated starches. Therefore, when retrograded under the same conditions and times, sonicated starches always reported higher relative crystallinity (by approximately 2–3%) compared with non-sonicated starches

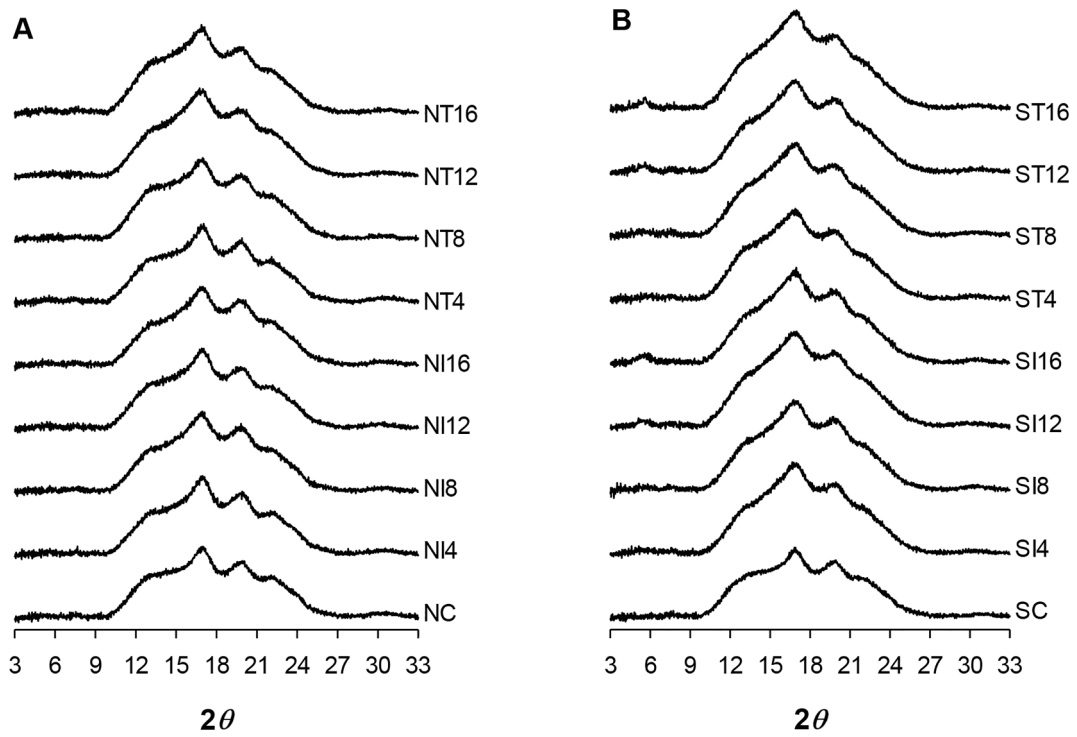

Fig. 3. Comparison of X-ray diffraction patterns of (A) non-sonicated and (B) sonicated high-amylose corn starches during retrogradation period. N, non-sonicated high-amylose corn starch; S, sonicated high-amylose corn starch; C, control (freshly gelatinized); Ix, stored under isothermal conditions for x days; Tx, stored under temperature-cycling conditions for x days.

(Table 3). In addition, temperature-cycled retrogradation induced higher relative crystallinity than isothermal storage, which corresponded with the results of DSC and Avrami kinetics analyses.

3.5. Effects of sonication on RS content of high-amylose corn starch

Kaur and Gill [25] reported an increase in rapidly digestible starch (RDS) and RS with a decrease in SDS after sonication of various cereal starches. It seems that an increase in porosity induces an increase in RDS, and disruption of the amorphous region may induce a slight increase in RS. Ding, Luo and Lin [24] also reported the changes in RS content after sonication of RS type 3 (retrograded starch), based on the different degree of molecular realignment according to the different ultrasonic power. However, as the type of starch and the sonication conditions were different in this study, the RS content of SC starch was not significantly different to that of NC starch (Table 4). High-amylose corn starch is a representative of RS type 2, because of its numerous α-1,4 glycosidic linkages of linear configuration and B-type crystals, which make it inaccessible to digestive enzymes [7,9]. In addition, the innate amylose–lipid complex therein contributes to the inherent RS5. Therefore, RS in NC and SC samples seemed to be mainly composed of RS2 and RS5.

Table 4
Changes in resistant starch content in non-sonicated and sonicated high-amylose corn starches during retrogradation.

Sample	Resistant starch (%)	Sample	Resistant starch (%)	*t*-test
NC	15.80 ± 0.26^{e}	SC	15.05 ± 0.61^{e}	n.s.
NI4	21.96 ± 0.64^{d}	SI4	28.93 ± 0.79^{d}	*
NI8	24.63 ± 0.77^{bc}	SI8	33.47 ± 1.35^{c}	*
NI12	25.38 ± 1.03^{b}	SI12	36.07 ± 1.00^{bc}	*
NI16	25.96 ± 0.75^{b}	SI16	37.91 ± 0.76^{b}	*
NT4	22.80 ± 0.68^{cd}	ST4	33.68 ± 1.13^{c}	*
NT8	25.40 ± 0.49^{b}	ST8	38.27 ± 1.10^{b}	*
NT12	29.11 ± 0.81^{a}	ST12	41.28 ± 0.35^{a}	*
NT16	30.63 ± 1.07^{a}	ST16	42.69 ± 0.80^{a}	*

N, non-sonicated high-amylose corn starch; S, sonicated high-amylose corn starch; C, control (freshly gelatinized); Ix, stored under isothermal conditions for x days; Tx, stored under temperature-cycling conditions for x days.
Values with different superscripts in the same column are significantly different ($p \leq 0.05$, Tukey's HSD test).
An asterisk (*) indicates a significant difference between starches retrograded isothermally and with temperature cycling under the same conditions ($p \leq 0.05$, *t*-test).

RS content increased as a function of retrogradation time, regardless of sonication, which could be explained by the development of RS3 during retrogradation. Although retrogradation increased RS content in both starches, sonicated starches always showed a higher RS content than non-sonicated starches after the same time of retrogradation. Therefore, sonication seemed to be advantageous for increasing RS content. As described above, sonication accelerated the retrogradation of starch molecules and the formation of a more crystalline structure. The short linear chains induced by sonication could be easily rearranged and this increased the rate of nucleation in sonicated starch, which was the most important factor to overcome the rate-limiting step of retrogradation. Numerous amylose nuclei and a dense arrangement of amylopectin contributed to the acceleration of RS formation via retrogradation in sonicated starch. Independent of sonication, starches that underwent temperature-cycled retrogradation showed a higher RS content than isothermally retrograded starches during the same storage period. This may be due to accelerated retrogradation, because stepwise nucleation and propagation could occur with temperature-cycled retrogradation between T_g and T_m, as stated above. In order to have an RS content of approximately 30%, non-sonicated starch had to be stored for 12 days under temperature cycling condition but the storage for 4 days under isothermal condition was enough for sonicated starch to have the similar RS content. It was clear that the sonication of starch simplified the process and shortened the amount of time required to produce RS. The greatest amount of RS was obtained when sonicated starch was stored under temperature-cycling conditions for 12 days.

4. Conclusions

Overall, the experimental data generated in the present study showed that sonication could induce appropriate structural properties for retrogradation, by reducing the molecular weight of amylopectin and amylose. In addition, temperature-cycling conditions were more effective than isothermal storage at inducing changes in retrogradation and structural characteristics for increasing RS content. This study contributes to a deeper understanding of the structural alterations that occur in starch after sonication and the impact of these changes on retrogradation behavior. Moreover, these findings suggest alternative applications of sonicated starch as a health-functional ingredient containing high RS content, and that the use of sonication can be extended to the health food industry, beyond food processing and preservation. Considering that intentional retrogradation is a tool for the generation of RS, sonication can be an effective strategy for achieving a targeted amount of RS. Optimization of the sonication treatment conditions for retrogradation, including frequency, power, and amplitude, is required to obtain a desirable amount of RS. In addition, dual modification by sonication and retrogradation may also be applied to other starches from different botanical sources containing various ratios of amylose and amylopectin.

CRediT authorship contribution statement

Kyu Tae Han: Conceptualization, Investigation, Visualization. **Ha Ram Kim:** Writing - original draft, Funding acquisition. **Tae Wha Moon:** Supervision, Funding acquisition. **Seung Jun Choi:** Supervision, Writing - review & editing.

Declaration of Competing Interest

The authors declare that they have no known competing financial interests or personal relationships that could have appeared to influence the work reported in this paper.

Acknowledgement

This work was supported with the partial support of “Main Research Program (E0211701) of the Korea Food Research Institute (KFRI) funded by the Ministry of Science and ICT, and with partial support of “the National Research Foundation of Korea (NRF) grant (No. NRF-2014R1A2A1A11050918)” funded by the Ministry of Science, ICT, and Future Planning.

Appendix A. Supplementary data

Supplementary data to this article can be found online at https://doi.org/10.1016/j.ultsonch.2021.105650.

References

[1] H. Inaba, Y. Hatanaka, T. Adachi, Y. Matsumura, T. Mori, Changes with retrogradation of mechanical and textural properties of gels from various starches, Carbohydr. Polym. 24 (1994) 31–40.
[2] H. Fredriksson, J. Silverio, R. Andersson, A.-C. Eliasson, P. Åman, The influence of amylose and amylopectin characteristics on gelatinization and retrogradation properties of different starches, Carbohydr. Polym. 35 (1998) 119–134.
[3] X. Zhou, R. Wang, S.H. Yoo, S.T. Lim, Water effect on the interaction between amylose and amylopectin during retrogradation, Carbohydr. Polym. 86 (2011) 1671–1674.
[4] J. Silverio, H. Fredriksson, R. Andersson, A.-C. Eliasson, P. Åman, The effect of temperature cycling on the amylopectin retrogradation of starches with different amylopectin unit-chain length distribution, Carbohydr. Polym. 42 (2000) 175–184.
[5] M.J. Miles, V.J. Morris, P.D. Orford, S.G. Ring, The roles of amylose and amylopectin in the gelation and retrogradation of starch, Carbohydr. Res. 135 (1985) 271–281.
[6] R.C. Eerlingen, M. Crombez, J.A. Delcour, Enzyme-resistant starch. I. Quantitative and qualitative influence of incubation time and temperature of autocalved starch on resistant starch formation, Cereal Chem. 70 (1993) 339–344.
[7] M.G. Sajilata, R.S. Singhal, P.R. Kulkarni, Resistant starch-a review, Compr. Rev. Food Sci. Food Saf. 5 (1) (2006) 1–17.
[8] H.N. Englyst, S.M. Kingman, J.H. Cummings, Classification and measurement of nutritionally important starch fractions, Eur. J. Clin. Nutr. 46 (1992) S33–50.
[9] D.F. Birt, T. Boylston, S. Hendrich, J.L. Jane, J. Hollis, L. Li, J. McClelland, S. Moore, G.J. Phillips, M. Rowling, K. Schalinske, M.P. Scott, E.M. Whitley, Resistant starch: promise for improving human health, Adv. Nutr.: Int. Rev. J., 4 (2013) 587-601.
[10] Y.Y. Xie, X.P. Hu, Z.Y. Jin, X.M. Xu, H.Q. Chen, Effect of temperature-cycled retrogradation on in vitro digestibility and structural characteristics of waxy potato starch, Int. J. Biol. Macromol. 67 (2014) 79–84.
[11] A.P. Nugent, Health properties of resistant starch, Nutr. Bull. 30 (2005) 27–54.
[12] A. Sharma, B.S. Yadav, B.Y. Ritika, Resistant starch: physiological roles and food applications, Food Rev. Int. 24 (2008) 193–234.
[13] J. Hasjim, S.O. Lee, S. Hendrich, S. Setiawan, Y. Ai, J.L. Jane, Characterization of a novel resistant-starch and its effects on postprandial plasma-glucose and insulin responses, Cereal Chem. 87 (2010) 257–262.
[14] J.A. Higgins, Resistant starch: metabolic effects and potential health benefits, J. AOAC Int. 87 (2004) 761–768.
[15] N. Masina, Y.E. Choonara, P. Kumar, L.C. du Toit, M. Govender, S. Indermun, V. Pillay, A review of the chemical modification techniques of starch, Carbohydr. Polym. 157 (2017) 1226–1236.
[16] R.N. Tharanathan, Starch-value addition by modification, Crit. Rev. Food Sci. Nutr. 43 (2005) 371–384.
[17] A. Patist, D. Bates, Ultrasonic innovations in the food industry: From the laboratory to commercial production, Innov. Food Sci. Emerg. Technol. 9 (2) (2008) 147–154.
[18] J. Zheng, Q. Li, A. Hu, L. Yang, J. Lu, X. Zhang, Q. Lin, Dual-frequency ultrasound effect on structure and properties of sweet potato starch, Starch – Stärke 65 (2013) 621–627.
[19] M. Sujka, J. Jamroz, Ultrasound-treated starch: SEM and TEM imaging, and functional behaviour, Food Hydrocolloids 31 (2013) 413–419.
[20] G.L. Peres, D.C. Leite, N.P.D. Silveira, Ultrasound effect on molecular weight reduction of amylopectin, Starch - Stärke 67 (2015) 407–414.
[21] A.J. Vela, M. Villanueva, Á.G. Solaesa, R. Ronda, Impact of high-intensity ultrasound waves on structural, functional, thermal and rheological properties of rice flour and its biopolymers structural features, Food Hydrocolloids 113 (2021), 106480.
[22] H. Wang, K. Xu, Y. Ma, Y. Liang, H. Zhang, L. Chen, Impact of ultrasonication on the aggregation structure and physicochemical characteristics of sweet potato starch, Ultrason. Sonochem. 63 (2020), 104868.
[23] A.P. Bonto, R.N. Tiozon Jr, N. Sreenivasulu, D.H. Camacho, Impact of ultrasonic treatment on rice starch and grain functional properties: a review, Ultrason. Sonochem. 71 (2021) 105383, https://doi.org/10.1016/j.ultsonch.2020.105383.
[24] Y. Ding, F. Luo, Q. Lin, Insights into the relations between the molecular structures and digestion properties of retrograded starch after ultrasonic treatment, Food Chem. 294 (2019) 248–259.
[25] H. Kaur, B.S. Gill, Effect of high-intensity ultrasound treatment on nutritional, rheological and structural properties of starches obtained from different cereals, Int. J. Biol. Macromol. 126 (2019) 367–375.
[26] S. Boufi, S. Bel Haaj, A. Magnin, F. Pignon, M. Imperor-Clerc, G. Mortha, Ultrasonic assisted production of starch nanoparticles: structural characterization and mechanism of disintegration, Ultrason. Sonochem. 41 (2018) 327–336.
[27] Y. Qin, L. Xue, Y. Hu, C. Qiu, Z. Jin, X. Xu, J. Wang, Green fabrication and characterization of debranched starch nanoparticles via ultrasonication combined with recrystallization, Ultrason. Sonochem. 66 (2020), 105074.
[28] A.F.K. Minakawa, P.C.S. Faria-Tischer, S. Mali, Simple ultrasound method to obtain starch micro- and nanoparticles fromcassava, corn and yam starches, Food Chem. 283 (2019) 11–18.
[29] W. Zhang, D.S. Jackson, Retrogradation behavior of wheat starch gels with differing molecular profiles, J. Food Sci. 57 (6) (1992) 1428–1432.
[30] S. Kitamura, K. Hakozaki, T. Kuge, Effects of molecular weight on the retrogradation of amylose, in: K. Nishinari, E. Doi (Eds.) Food Hydrocolloids, Springer US, New York, 1994, pp. 179-182.
[31] F. Zhu, Impact of ultrasound on structure, physicochemical properties, modifications, and applications of starch, Trends Food Sci. Technol. 43 (2015) 1–17.
[32] T. Jankowski, C.K. Rha, Retrogradation of starch in cooked wheat, Starch – Stärke 38 (1986) 6–9.
[33] Z. Luo, X. Fu, X. He, F. Luo, Q. Gao, S. Yu, Effect of ultrasonic treatment on the physicochemical properties of maize starches differing in amylose content, Starch – Stärke 60 (2008) 646–653.
[34] R. Czechowska-Biskup, B. Rokita, S. Lotfy, P. Ulanski, J.M. Rosiak, Degradation of chitosan and starch by 360-kHz ultrasound, Carbohydr. Polym. 60 (2005) 175–184.
[35] D. Voet, J.G.P. Voet, W. Charlotte, G.V. Judith, W.P. Charlotte, Fundamentals of Biochemistry: Life at the Molecular Level, Wiley, New York, 2013.
[36] R. Hoover, Acid-treated starches, Food Rev. Int. 16 (2000) 369–392.
[37] C.G. Biliaderis, T.J. Maurice, J.R. Vose, Starch gelatinization phenomena studied by differential scanning calorimetry, J. Food Sci. 45 (1980) 1669–1674.
[38] A. Lopez-Rubio, B.M. Flanagan, E.P. Gilbert, M.J. Gidley, A novel approach for calculating starch crystallinity and its correlation with double helix content: a combined XRD and NMR study, Biopolymers 89 (2008) 761–768.
[39] S. Wang, C. Li, L. Copeland, Q. Niu, S. Wang, Starch retrogradation: a comprehensive review, Compr. Rev. Food Sci. Food Saf. 14 (5) (2015) 568–585.
[40] E.A. Arık Kibar, İ. Gönenç, F. Us, Modeling of retrogradation of waxy and normal corn starches, Int. J. Food Prop. 14 (2011) 954–967.

[41] M.A. Ottenhof, I.A. Farhat, Starch retrogradation, Biotechnol. Genet. Eng. Rev. 21 (2004) 215–228.
[42] R.G. McIver, D.W.E. Axford, K.H. Colwell, G.A.H. Elton, Kinetic study of the retrogradation of gelatinised starch, J. Sci. Food Agric. 19 (1968) 560–563.
[43] K.M. Chung, T.W. Moon, H. Kim, J.K. Chun, Physicochemical properties of sonicated mung bean, potato, and rice starches, Cereal Chem. 79 (2002) 631–633.
[44] A.M. Amini, S.M.A. Razavi, S.A. Mortazavi, Morphological, physicochemical, and viscoelastic properties of sonicated corn starch, Carbohydr. Polym. 122 (2015) 282–292.
[45] I.L. Herceg, A.R. Jambrak, D. Šubarić, M. Brnčić, S.R. Brnčić, M. Badanjak, B. Tripalo, D. Ježek, D. Novotni, Z. Herceg, Texture and pasting properties of ultrasonically treated corn starch, Czech J. Food Sci. 28 (2010) 83–93.
[46] J. Jin, H. Lin, A.E.A. Yagoub, S. Xiong, L. Xu, C.C. Udenigwe, Effects of high power ultrasound on the enzymolysis and structures of sweet potato starch, J. Sci. Food Agric. 100 (2020) 3498–3506.
[47] H.R. Kim, S.J. Choi, H.D. Choi, C.S. Park, T.W. Moon, Amylosucrase-modified waxy potato starches recrystallized with amylose: the role of amylopectin chain length in formation of low-digestible fractions, Food Chem. 318 (2020) 126490, https://doi.org/10.1016/j.foodchem.2020.126490.